Modelling of the elastic parameters development of an oilwell cement paste at a very early age under downhole conditions

M. Bourissai[1,2], F. Meftah[1], N. Brusselle-Dupend[2] & G. Bonnet[1]
[1]*Université Paris-Est, MSME, Marne la Vallée, France*
[2]*IFP, Rueil-Malmaison, France*

Abstract

The characterisation and modelling of the mechanical behaviour of an oilwell cement paste at a very early age (≤24h) under high pressure and elevated temperature are studied. A multiscale homogenization approach is adopted. For this purpose, the evolution of the volume fractions of the different phases of the cement was determined by means of a kinetics model for the four main hydration reactions of a class G oilwell cement. Calorimetric experiments were performed in order to be compared with the results of the used kinetics model, on the one hand, and to study pressure and temperature effect on the hydration kinetics, on the other hand. A homogenization model is presented in order to predict the bulk and shear moduli evolutions. The model-based results are in agreement with dynamic moduli measurements data from ultrasonic propagation.

Keywords: cement paste, hydration, multiscale homogenization.

1 Introduction

In constructing oil and gas wells, primary cementing technique is used for placing cement slurries in the annular space between the drilled rock formation and the steel casing. The cement then hardens to form a hydraulic seal preventing the migration of formation fluids in the annulus. This later has to be especially well cemented because the cement sheath is submitted to various thermal and mechanical loadings from the drilling phase to the abandon phase. Over the past ten years, several papers concerned with the long-term mechanical durability of the cement sheath. However, until now there are no physical and mechanical inputs that permit to evaluate the development of stresses and strains at a very

WIT Transactions on Engineering Sciences, Vol 64, © 2009 WIT Press
www.witpress.com, ISSN 1743-3533 (on-line)
doi:10.2495/MC090341

early age during cement paste hydration in oil or gas wells [1–4]. The monitoring of the mechanical properties measurements of the cement paste at a very early age under downhole conditions (elevated temperature (HT) and high pressure (HP)) is not trivial due to the lack of instrumentation that can cure and maintain the cement paste under HTHP conditions while testing for mechanical properties. The present work aims to characterise and model the mechanical behaviour of a class G oilwell cement paste at a very early age curing under downhole conditions.

The first part of this paper concerns the homogenization of the mechanical behaviour of the cement paste at a very early age. The volume fractions evolution of the different phases of the cement paste are determined from a cement hydration kinetics model for the four anhydrous cement components. The evolution of the elastic properties at a very early age can be estimated by using an upscaling approach that provides access to the macroscopic behaviour from the intrinsic behaviour of the components at the first scale and their volume fractions.

The second part deals with the experimental characterisation of the oilwell cement paste. Semi-adiabatic calorimetric measurement is presented in order to be compared with the used kinetics model. Isotherm calorimetric measurements under HP were also conducted to study downhole conditions effect on hydration kinetics. Dynamic moduli obtained by ultrasonic propagation are finally compared with the homogenization model-based results.

2 Homogenization model

Several homogenization modelling approaches of the elastic behaviour of concrete were proposed [5–7] based on the knowledge of the elastic properties and volume fractions of its constituents (fig. 1) either during the hydration or in post-hydration phase. The predictive capabilities of these upscaling approaches to determine the macroscopic elastic properties seem to be well-established [5, 6].

The extension of such approaches to the prediction of the isothermal and no ageing viscoelastic behaviour of concrete to estimate its creep in post-hydration was also proposed from the use of the correspondence principle based on the Laplace-Carson transformation (Le *et al.* [7]). But this principle cannot be applied on the hydrating cement paste because of the evolving hydrate phase viscoelasticity and exothermic reactions in progress. The approach is consequently limited to the instantaneous elastic properties of the cement paste. However in this work, in contrast to previous studies [5, 6], the aqueous phase is taken into account to predict these properties. At a very early age, this phase has an important role and it cannot be occulted. This analysis appears to be essential from the beginning of the hydration and until the solid skeleton becomes sufficiently rigid to induce a cavitation of the aqueous phase in the capillary porosity.

In this contribution, the study is particularly focused on the instantaneous properties of the cement paste during hydration by the choice of a microstructure model and a given homogenization schema.

2.1 Schematization of the cement paste microstructure during hydration

When anhydrous cement is mixed with water, the cement paste can be regarded at a very early age as a suspension with a geometrical percolation (existence of a non-cohesive solid skeleton) of the anhydrous cement grains due to their sedimentation. Thereafter, the hydration leads to the nucleation and the growth of a multi-components and porous hydrate phase, which involves a gradual increase of the mechanical properties of the hardening cement paste (a mechanical percolation due to the development of a cohesive solid skeleton). The progressive development of the hydrated compounds induces a gradual decrease of the aqueous and anhydrous phases (fig. 2). After a certain time, the aqueous phase is mainly present in a filled or partially filled (due to water cavitation) porosity, drowned in the hydrate phase.

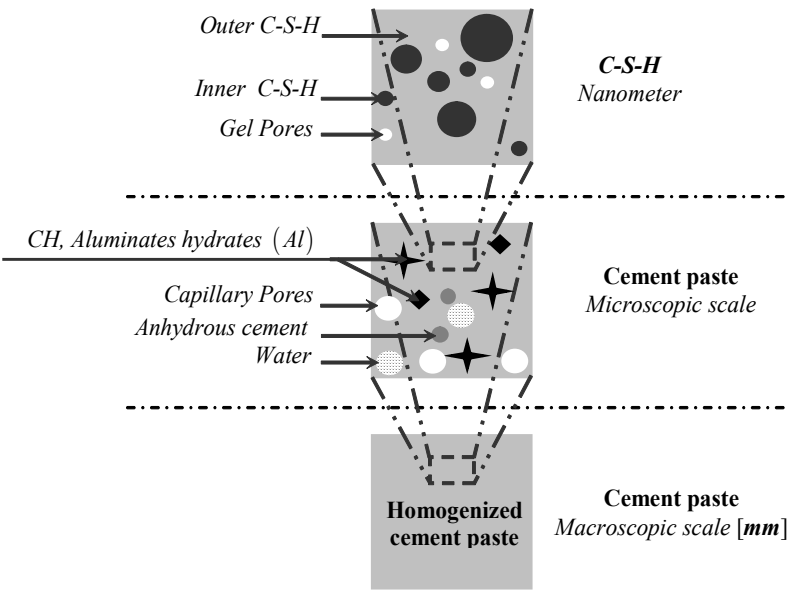

Figure 1: Upscaling method applied to cement paste.

Accordingly, the schematization of the evolutionary microstructure of the cement paste during hydration is not trivial. Nevertheless, the representation of this microstructure is necessary to estimate the homogenized mechanical properties. In this work, the adopted microstructure schematization is given in fig. 3 with the three main involved phases: anhydrous grains, aqueous phase and developed hydrates with an embedded gel porosity. The aqueous phase is assumed to initially surround the anhydrous phase (suspension) and

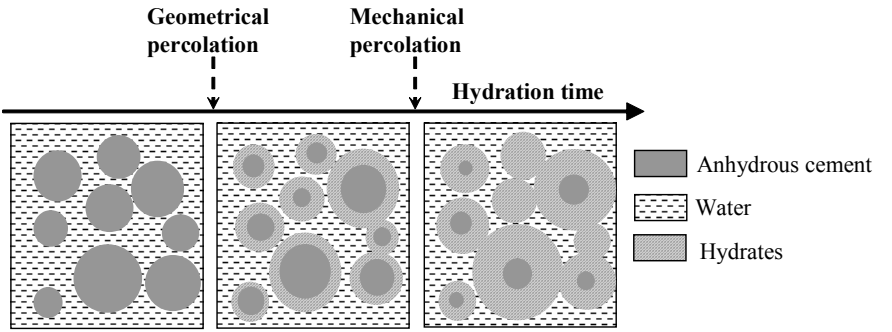

Figure 2: Cement paste phases evolution during early age hydration.

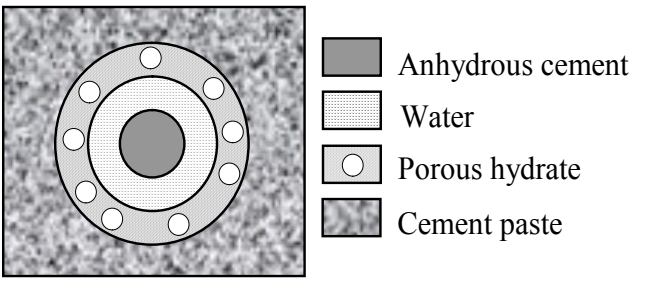

Figure 3: Schematization of the cement paste microstructure at a very early age after the mechanical percolation threshold.

progressively to be coated by the formed hydrate, this latter giving rise to a connected cohesive skeleton (fig. 2). Therefore, this schematic representation of the cement paste can cover all the hydration process (from suspension to mechanical percolation).

2.2 Retained homogenization schema

To determine the macroscopic elastic properties (bulk and shear moduli) of the adopted microstructure, a suitable homogenization schema is needed. For this purpose, Mori-Tanaka or the classic self-consistent schema do not seem to be adapted for the evolutionary microstructure of cement paste. The first one requires that one phase remains a dominant connected matrix, whereas none of the cement paste phases keeps this property during hydration. The second schema is more adapted to describe the percolation of one phase from an initial medium where all phases are equi-present. The initial phase concentrations show that the initial state is beyond the threshold of percolation. Accordingly, the generalised self-consistent schema is adopted here which ensures a continuous description of the evolution of the microstructure during hydration. For this purpose (fig. 4), n isotropic elastic phases are represented by concentric inclusions embedded in the effective medium (n+1). Each phase i is

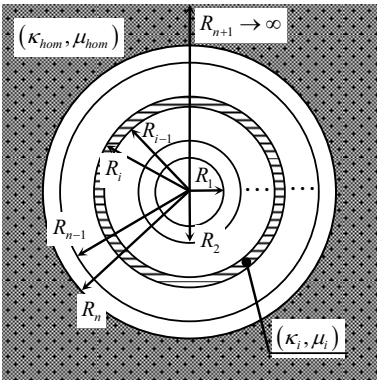

Figure 4: Generalized schema of a multiphase medium according to [8].

characterised by its bulk and shear moduli (κ_i, μ_i) and its volume fraction $f_i = \left(R_i^3 - R_{i-1}^3\right)/R_n^3$. This representation corresponds to a medium where the phases are distributed in a completely isotropic and random way.

For this schema, the homogenized bulk and shear moduli κ_{hom} and μ_{hom} are respectively given by [8]:

$$\kappa_{hom} = \kappa_n - \frac{\left(3\kappa_n + 4\mu_n\right)Q_{21}^{(n-1)}}{3\left(Q_{11}^{(n-1)}R_n^3 + Q_{21}^{(n-1)}\right)} \tag{1}$$

$$\mu_{hom} = \frac{-B \pm \sqrt{B^2 - 4AC}}{2A}\mu_n \tag{2}$$

where the matrix $Q^{(n-1)}$ and the terms coefficients *A*, *B*, and *C* are given in [8]. Eqns (1) and (2) are then applied to the retained microstructure with $n = 3$. Consequently, the three phases contribute in the estimation of the homogenized bulk modulus κ_{hom} through their volume fractions and their elastic properties except the shear modulus of the anhydrous cement phase μ_a:

$$\kappa_{hom} = \kappa_{hom}\left(f_w, \kappa_w, f_a, \kappa_a, \overline{\kappa}_h, \overline{\mu}_h\right) \tag{3}$$

where $\kappa_w, \kappa_a, \overline{\kappa}_h, \overline{\mu}_h$ are respectively the elastic properties of the aqueous phase, the anhydrous grains and the formed porous hydrate and $f_w, f_a, \overline{f}_h = 1 - f_w - f_a$ denote the corresponding volume fractions. As concerns the homogenized shear modulus μ_{hom}, the aqueous and anhydrous cement phase contribute only by their volume fractions and act as a void. Indeed, hydrate-water interface withstands no tangential stress when sheared [8].

3 Material input parameters

The homogenized bulk and shear moduli $(\kappa_{hom}, \mu_{hom})$ for the cement paste during hydration require to know the intrinsic elastic moduli of the cement paste components at the first scale and their volume fractions evolution during hydration. The mechanical and chemical inputs are detailed below.

3.1 Mechanical data

The hydrate phase illustrated in fig. 2 represents all forming hydrates which are first homogenized. Indeed the elastic properties of this hydrate phase (κ_h, μ_h) are determined by a mixture law of the elastic properties of each hydrate component (κ_y, μ_y) with y = *C-S-H, CH and Aluminates hydrates* (Al).

The same approach is adopted to determine the elastic properties of the anhydrous cement (κ_a, μ_a) from the elastic properties of each anhydrous component (κ_x, μ_x) with $x = C_3S$, C_2S, C_3A and C_4AF.

$$(\kappa_h, \mu_h) = \sum_y \hat{f}_y(t)(\kappa_y, \mu_y) \tag{4}$$

$$(\kappa_a, \mu_a) = \sum_x \hat{f}_x(t)(\kappa_x, \mu_x) \tag{5}$$

where $\hat{f}_y$ is the volume fraction of each hydrated component in the hydrate phase and $\hat{f}_x$ is the volume fraction of each anhydrous component in the anhydrous cement phase.

The bulk modulus of the aqueous phase is considered equal to $\kappa_w = 2{,}2\ GPa$.

The intrinsic elastic properties $(\kappa_x,\ \mu_x,\ \kappa_y,\ \mu_y)$ are calculated using the following expressions:

$$\kappa = \frac{E}{3(1-2\nu)};\ \mu = \frac{E}{2(1+\nu)} \tag{6}$$

the Young modulus E and the Poisson's ratio ν values for the cement paste components are presented in table 1.

Table 1: Intrinsic elastic properties of the cement paste components [5].

	Anhydrous cement components: *x*				Hydrates: *y*		
	C_3S	C_2S	C_3A	C_4AF	*C-S-H*	*CH*	*Al*
E[GPa]	135	140	145	125	24	38	24
ν [–]	0.3	0.3	0.3	0.3	0.24	0.3	0.24

Then the generalized self-consistent schema is first used for two phases ($n = 2$) to estimate the elastic properties of the hydrate taking into account the gel porosity created during hydration $(\bar{\kappa}_h, \bar{\mu}_h)$. Then the outputs $(\kappa_a, \kappa_w, \bar{\kappa}_h, \bar{\mu}_h)$ become inputs in the cement paste homogenization schema as illustrated in fig. 3.

3.2 Chemical data

The second set of inputs concerns the determination of the volume fractions evolution occupied by the different phases in the hydrating cement paste.

This requires two steps: (1) the description of the hydration degree evolution of each chemical reaction from kinetic laws and (2) the determination of the volume fractions evolution of each phase of the cement paste during hydration.

3.2.1 Hydration model

In this subsection, the kinetic laws using chemical affinity are used for the description of cement hydration kinetics [5]. These kinetic laws were found useful for the prediction of the cement hydration during all hydration stages and easily incorporated within the framework of the porous medium chemically reactive (Ulm *et al.* [9]). Therefore, the cement hydration kinetic reads:

$$\frac{d\xi_x}{dt} = \frac{1}{\tau_x(T,\phi)}\tilde{A}(\xi_x) \tag{7}$$

where $\tilde{A}[-]$ is the normalized chemical affinity, $\tau_x[h]$ denotes the characteristic time of the chemical reaction, which depends on temperature $T[K]$, blaine fineness ϕ $[cm^2.g^{-1}]$, the type of clinker mineral and water/cement (w/c) ratio.

The concept of reaction dependence on temperature is well described by the Arrhenius equation (Pichler and Coussy [10]):

$$\tau_x(T,\phi) = \tau_x(T_0)\frac{\phi_0}{\phi}exp\left(\frac{E_a^x}{R}\left(\frac{1}{T}-\frac{1}{T_0}\right)\right) \tag{8}$$

where $\tau_x(T_0)$ is the characteristic time of the chemical reaction [5] with $T_0 = 293\ K$, $\phi_0 = 3602\ cm^2.g^{-1}$ is the reference fineness and ϕ is the fineness of the used cement.

As illustrated in fig. 6a, three stages are observed during cement hydration: (1) dissolution of clinker (induction stage), (2) nucleation accompanied by reactions acceleration and formation of hydration products (growth stage) and (3) finally hydration controlled by dissolved ions diffusion through a thickening layer of hydration products to the anhydrous cement grain (diffusion stage).

The normalized affinity consequently takes a particular expression according to the stage similarly to [5].

Finally the overall hydration degree $\xi(t)$ is obtained from the values of the partial hydration degree $\xi_x(t)$ of each anhydrous cement component x determined from the kinetic laws as follows:

$$\xi(t) = \frac{\sum_x m_x^0 \xi_x(t)}{m_a^0} = \sum_x f_x^m \xi_x(t) \tag{9}$$

where m_x^0 is the initial mass of the anhydrous cement component x, $m_a^0 = \sum_x m_x^0$ is the initial total mass of the anhydrous cement and f_x^m is the initial mass fraction of the anhydrous components.

As $\xi(t)$ will be obtained by calorimetric measurement (semi-adiabatic), an alternative relation to eqn (9) is proposed in eqn (10):

$$\xi(t) = \frac{\mathrm{Q(t)}}{\mathrm{Q}^\infty} = \frac{\sum_x f_x^m q_x^\infty \xi_x(t)}{\sum_x f_x^m q_x^\infty} \tag{10}$$

where $\mathrm{Q(t)}$ is the heat of hydration, Q^∞ is the asymptotic hydration heat $(\xi = 1)$ and q_x^∞ is the asymptotic heat hydration of each component x.

Note that $\mathrm{Q(t)}$ depends on the used q_x^∞ values taken into account (table 2).

Table 2: Values of hydration heat for each component x at $\xi = 1$.

	The Heat of hydration ($J.g^{-1}$)			
	$q_{C_3S}^\infty$	$q_{C_2S}^\infty$	$q_{C_3A}^\infty$	$q_{C_4AF}^\infty$
Taylor [11]	517	262	1144	418
Chougnet [12]	520	70	1670	725

3.2.2 Volume fractions evolution during hydration

The hydration kinetics for each anhydrous cement component is used to determine the volume fractions evolution of the different phases of the cement paste during hydration.

At each time *t,* the volumes of remaining anhydrous cement V_a and water V_w and the formed volumes of hydrates V_h and gel porosity V_p are determined. The volume of the cement paste V_c is then given by:

$$V_c(t) = V_a(t) + V_w(t) + V_h(t) + V_p(t) \tag{11}$$

In this work, the cement paste volume is assumed constant during hydration:

$$V_c(t) = V_c^0 = V_a^0 + V_w^0 \tag{12}$$

where V_a^0 and V_w^0 are the initial volumes of anhydrous cement and water in the mix.

The volume fractions for each phase of the cement paste can be formulated as:

$$f_a(t) = \frac{V_a(t)}{V_c^0} \;;\; f_w(t) = \frac{V_w(t)}{V_c^0} \;;\; f_h(t) = \frac{V_h(t)}{V_c^0} \;;\; f_p(t) = \frac{V_p(t)}{V_c^0} \tag{13}$$

with:

$$f_a(t) + f_w(t) + f_h(t) + f_p(t) = 1 \tag{14}$$

Then, based on the stoechimetric ratio of the chemical reactions (θ) for the four main components of the cement, the molar masses (M) and densities (ρ) of

the different phases, the volume fractions of the different phases $f_a(t)$, $f_w(t)$, $f_p(t)$ and $f_h(t)$ can be determined according to [5] versus the hydration degree $\xi_x(t)$.

The volume fractions of the different phases of the cement paste are then formulated as:

$$f_a(t) = f_a^0 \sum_x (1 - \xi_x(t)) f_x^0 \frac{\rho_x}{\rho_a} \tag{15}$$

$$f_w(t) = f_w^0 - f_a^0 \sum_x \left(\theta_w^x f_x^0 \frac{\rho_x}{\rho_w} \frac{M_w}{M_x} \xi_x(t) \right) \tag{16}$$

$$f_p(t) = f_a^0 \sum_x \theta_p^x \frac{\rho_x}{\rho_a} f_x^0 \xi_x(t) \tag{17}$$

$$f_h(t) \begin{cases} f_{C-S-H;\,CH}(t) = f_a^0 \sum_y \left(\sum_x \theta_y^x \frac{M_y}{M_x} \frac{\rho_x}{\rho_h} f_x^0 \xi_x(t) \right) & (18) \\ f_{Al}(t) = 1 - f_a(t) - f_e(t) - f_p(t) - f_{C-S-H;CH}(t) & (19) \end{cases}$$

Fig. 5 shows the volume fractions evolution during the first 24 hours of the class G cement paste hydration. The volume fractions linearly evolve versus the overall hydration degree $\xi(t)$ determined from eqn (9). The consumption of the anhydrous cement and water during the hydration reactions results in the formation of hydrates and gel porosity which is estimated to be about 2% after 24 hours of hydration when the curing temperature is equal to 60°C (fig. 5b).

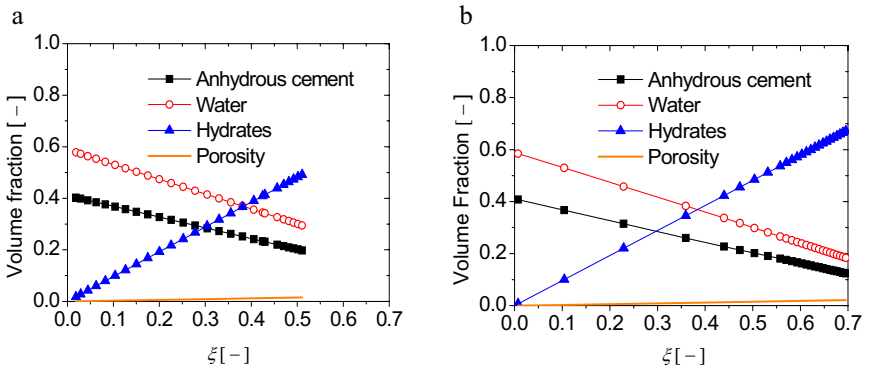

Figure 5: Volume fractions evolution of a class G cement paste components of w/c = 0.44 vs. the overall hydration degree at 23°C (a) and 60°C (b).

4 Cement paste characterisation

Experimental characterisation aims to provide data in order to be compared with the model-based results. Class G cement produced by Dyckerhoff which is considered a representative oilwell cement is used in this work. Its physical

Table 3: Physical properties and mineral compositions of the class G cement.

Physical properties	fineness ($cm^2.g^{-1}$)	3160
	grains average radium (cm)	9.4×10^{-4}
Mineral compositions	C_3S (% mass)	56
	C_2S (% mass)	25.7
	C_3A (% mass)	2
	C_4AF (% mass)	16.3

properties and mineral composition are given in table 3. The anhydrous cement was mixed with deionised water to prepare cement paste with w/c = 0.44.

4.1 Hydration characterisation

4.1.1 Isotherm calorimeter DSC

Calorimetric measurements were performed using isotherm calorimeter (HP micro DSC VII). Such calorimeter permits to study the temperature (T) and the pressure (P) effect on the hydration kinetics by following the heat flow emitted during cement paste hydration under downhole conditions. The tests conditions are summarized in table 4.

Table 4: Experimental conditions of DSC tests.

	Test 1	Test 2	Test 3	Test 4
T (°C)	23	23	60	60
P (Pa)	10^5	200×10^5	10^5	200×10^5

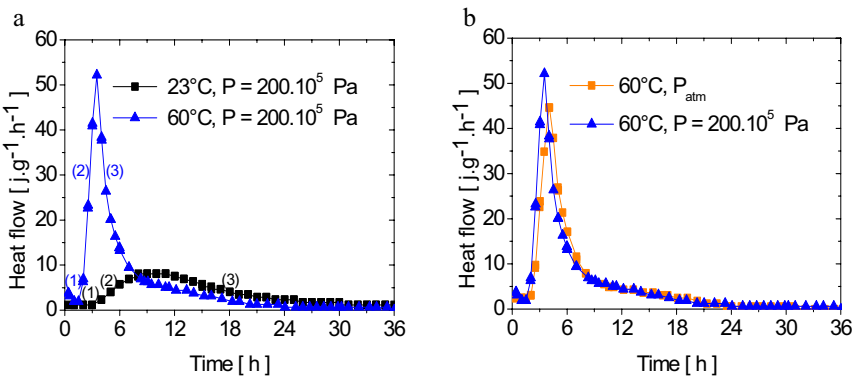

Figure 6: Heat flow per gram vs. the used cement paste (w/c=0.44) hydration time. Curing conditions: a. 23°C and 60°C under Nitrogen pressure equal to 200×10^5 Pa. b. 60°C under two different pressures: P_{atm} and 200×10^5 Pa.

Fig. 6a shows that when curing temperature is elevated (60°C), the three main phases of hydration duration are significantly reduced and the exothermic heat

flow peak is higher than the heat flow evolution at 23°C. Indeed, it is well known that the increase of curing temperature accelerates the hydration reactions of the cement paste [13, 14]. However, the effect of (P) on the hydration kinetics is by far less remarkable than the one of (T) (fig. 6b). The (P) effect is consequently assumed negligible in this work. For this reason, the pressure effect was not taken into account in the homogenization model.

4.1.2 Semi-adiabatic calorimeter

The Langavant semi-adiabatic calorimeter was used to quantify the heat emitted $Q(t)$ during the exothermic chemical reactions between anhydrous cement and water. Such calorimeter works only at atmospheric (P) and (T). The overall hydration degree is then calculated by using eqn (10) where $Q(t)$ is the measured hydration heat. The overall hydration degree obtained from semi-adiabatic measurement is in good agreement with the results of the used hydration model (fig. 7) obtained either from eqn (9) or from eqn (10).

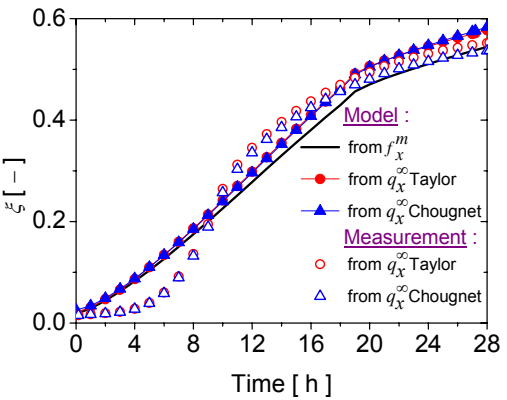

Figure 7: The overall hydration degree obtained from semi-adiabatic measurement compared with the used hydration model results at 23°C.

5 Modelling and experiment comparison

Fig. 8 shows that the homogenized elastic properties first gradually increase during the hydration of the class G oilwell cement paste then tend to stabilize from 20 hours at 23°C, and earlier from 8 hours at 60°C.

The comparison in fig. 6a between the model-based results and the dynamic elastic moduli measurements obtained by ultrasonic propagation at atmospheric conditions carried out on a white cement paste (PCCB9402) of w/c=0.4 [15] shows that the used model qualitatively describe the elastic mechanical properties evolution of the used cement paste.

Ultrasonic measurements and unconfined uniaxial compression tests are in progress on the studied cement paste curing at 23°C and 60°C in order to be compared with the homogenization model-based results.

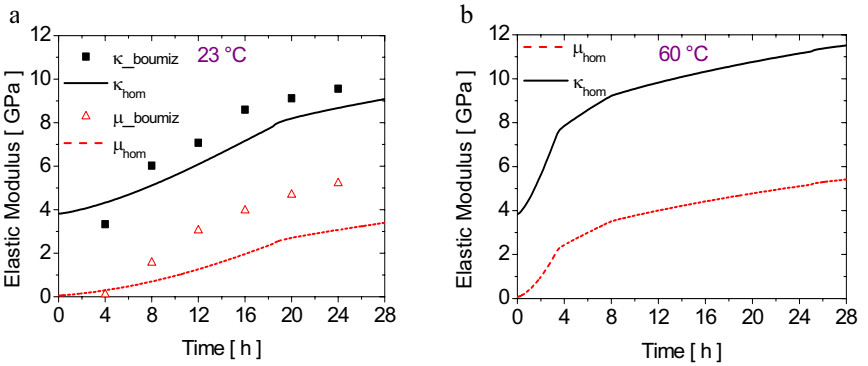

Figure 8: Elastic moduli evolution during cement paste hydration. a. Homogenized elastic moduli evolution compared with dynamic elastic moduli from ultrasonic measurements at atmospheric pressure [15]. b. Homogenized elastic moduli evolution at 60°C.

References

[1] Thiercelin, M.J., Dargaud, B., Baret, J.F., Rodriguez, W.J., Cement Design Based on Cement Mechanical Response, *SPE Annual Technical Conf. and Exhibition*, pp. 337-347, 1997.

[2] Bosma, M., Ravi,.K., Van Driel, W., Jan Schreppers, G., Design Approach to Sealant Selection for the Life of the Well,, *SPE Annual Technical Conf. and Exhibition*, pp.1-14, 1999.

[3] Di Lullo, G., Rae, P., Cements for Long Term Isolation – Design Optimization Computer Modelling and Prediction, *IADC/SPE Asia Pacific Drilling Technolog*, pp.1-14, 2000.

[4] Boukhelifa L., Moroni N., James S.G., Le Roy-Delage S., Thiercelin M.J., Lemaire G., Evaluation of Cement Systems for Oil and Gas Well Zonal Isolation in a Full-Scale Annular Geometry, *IADC/SPE Drilling Conf.*, pp. 44-53, 2004.

[5] Bernard, O., Ulm, F.-J., Lemarchand, E., Multiscale micromechanics-hydration model for the early-age elastic properties of cement-based materials, *Cement and Concrete Research*, 33 (9), pp. 1293-1309, 2003.

[6] Smilauer, V., *Elastic Properties of hydrating cement paste determined from hydration models*, PhD Thesis, Technical University in Prague, 2005.

[7] Le, Q.V., Meftah, F., He, Q.C., and Le-Pape, Y., Creep and relaxation functions of a heterogeneous viscoelastic porous medium using the Mori-Tanaka homogenization scheme and a discrete microscopic retardation spectrum, *Mechanics of Time Dependent Materials*, 11(3-4), pp 309-331, 2008.

[8] Hervé E. & Zaoui A., (1992), n-Layered inclusion-based micromechanical modelling, *Int. J. Engng. Sci.*, 31 (1), pp. 1-10, 1993.

[9] Ulm, F.-J, Coussy, O., Modeling of thermomechanical couplings concrete at early ages, *Journal of Engineering Mechanics*, 121(7), pp.785-794, 1995.
[10] Pichler, C., Lackner, R., and Mang, H. A., A multiscale micromechanics model for the autogenous-shrinkage deformation of early-age cement-based materials, *Engineering Fracture Mechanics*,74(1-2), pp.34-58, 2006.
[11] Taylor, H.F.W., *Cement chemistry*, Thomas Telford (eds), 1997.
[12] Chougnet, A., *Composites ciment/polymère : rhéologie, hydratation*. PhD Thesis, Bretagne Occidentale University, 2006.
[13] Escalante-Garcia, J.I. & Sharp, J.H., Effect of temperature on the hydration of the main clinker phases in Portland cements: Part I, neat cements. *Cement and Concrete Research*, 28 (9), pp. 1245-1257, 1998.
[14] Heikal, M., Morsy, M. S., Aiad, I., Effect of treatment temperature on the early hydration characteristics of superplasticized silica fume blended cement pastes, *Cement and Concrete Research*, 35(4), pp. 680-687,2005.
[15] Boumiz, A., Vernet, C. & Cohen-Tenoudji, F., Mechanical Properties of Cement Pastes and Mortars at Early ages, *Adv. Cem. Bas. Mat.*, 3, pp. 94-106, 1996.